AD-A113 660 PHILIPS LABS BRIARCLIFF MANOR NY F/G 13/1
CONTINUED DEVELOPMENT OF A 10 K CRYOGENIC COOLER.(U)
MAR 82 W NEWMAN N00014-81-C-0524
UNCLASSIFIED NL

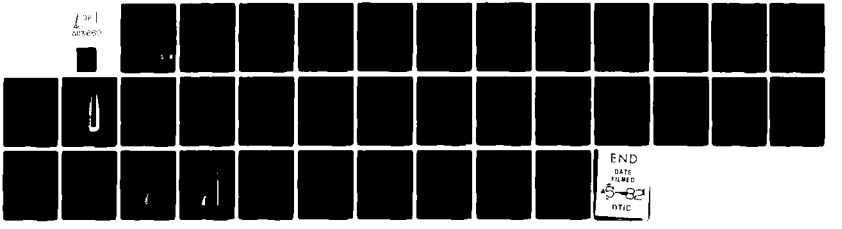

(12)

AD A113660

CONTINUED DEVELOPMENT OF A 10°K CRYOGENIC COOLER

PHILIPS LABORATORIES
A Division of North American Philips Corporation
Briarcliff Manor, New York 10510

March 1982

Final Report for Period 1 June - 31 December 1981

DTIC FILE COPY

OFFICE OF NAVAL RESEARCH
Department of the Navy
Arlington, Virginia 22217

UNCLASSIFIED

SECURITY CLASSIFICATION OF THIS PAGE *(When Data Entered)*

REPORT DOCUMENTATION PAGE		READ INSTRUCTIONS BEFORE COMPLETING FORM
1. REPORT NUMBER	2. GOVT ACCESSION NO. AD-A	3. RECIPIENT'S CATALOG NUMBER
4. TITLE *(and Subtitle)* CONTINUED DEVELOPMENT OF A 10°K CRYOGENIC COOLER		5. TYPE OF REPORT & PERIOD COVERED Final Technical Report 1 June - 31 December 1981
		6. PERFORMING ORG. REPORT NUMBER
7. AUTHOR(s) Wyatt Newman		8. CONTRACT OR GRANT NUMBER(s) N00014-81-C-0524
9. PERFORMING ORGANIZATION NAME AND ADDRESS PHILIPS LABORATORIES A Division of North American Philips Corp. Briarcliff Manor, New York 10510		10. PROGRAM ELEMENT, PROJECT, TASK AREA & WORK UNIT NUMBERS
11. CONTROLLING OFFICE NAME AND ADDRESS OFFICE OF NAVAL RESEARCH Department of the Navy Arlington, Virginia 22217		12. REPORT DATE March 1982
		13. NUMBER OF PAGES 37
14. MONITORING AGENCY NAME & ADDRESS(*if different from Controlling Office*)		15. SECURITY CLASS. (*of this report*) UNCLASSIFIED
		15a. DECLASSIFICATION/DOWNGRADING SCHEDULE

16. DISTRIBUTION STATEMENT *(of this Report)*

DISTRIBUTION STATEMENT A
Approved for public release;
Distribution Unlimited

17. DISTRIBUTION STATEMENT *(of the abstract entered in Block 20, if different from Report)*

18. SUPPLEMENTARY NOTES

19. KEY WORDS *(Continue on reverse side if necessary and identify by block number)*

Stirling cycle refrigerator
cryogenic refrigerator for 10°K
triple-expansion Stirling-cycle refrigerator
free-displacer, free-piston system
cryocooler for superconducting elements
linear motor

20. ABSTRACT *(Continue on reverse side if necessary and identify by block number)*

Development of the design selected for the 10°K cryogenic cooler in the Phase I study was continued in this second phase of the program. The configuration arrived at in Phase I was a triple-expansion, free-displacer Stirling-cycle refrigerator driven by a linear motor. Vibrations are attenuated with a passive vibration absorber. Electromagnetic noise from the motor is attenuated with layered, high permeability, magnetic shielding. The cooler can meet or better the goals for cooling and power consumption. It can provide 200 mW

(Continued)

DD FORM 1 JAN 73 1473 EDITION OF 1 NOV 65 IS OBSOLETE

UNCLASSIFIED

SECURITY CLASSIFICATION OF THIS PAGE *(When Data Entered)*

20 ABSTRACT (Cont'd)

of cold at 10°K at the maximum allowable input of 250 W, or provide the prescribed 50 mW of cold with less than 100 W of input power. The cooler weight is 35.9 kg for the thermodynamic components, 17 kg for the vibration absorber, and 8.6 kg for the EMI shielding. The design goals for cooldown time and regulation of the cold-tip temperature can be met or bettered. The resulting EMI and vibration levels can not be accurately predicted, but they are expected to exceed the extremely low levels desired.

SUMMARY

Development of the design selected for the 10°K cryogenic cooler in the Phase I study was continued in this second phase of the program. The configuration arrived at in Phase I was a triple-expansion, free-displacer Stirling-cycle refrigerator driven by a linear motor. Vibrations are attenuated with a passive vibration absorber. Electromagnetic noise from the motor is attenuated with layered, high permeability, magnetic shielding. The cooler can meet or better the goals for cooling and power consumption. It can provide 200 mW of cold at 10°K at the maximum allowable input of 250 W, or provide the prescribed 50 mW of cold with less than 100 W of input power. The cooler weight is 35.9 kg for the thermodynamic components, 17 kg for the vibration absorber, and 8.6 kg for the EMI shielding. The design goals for cooldown time and regulation of the cold-tip temperature can be met or bettered. The resulting EMI and vibration levels can not be accurately predicted, but they are expected to exceed the extremely low levels desired.

PREFACE

The author wishes to acknowledge the substantial technical contributions to this effort from several key people. Mr. Alexander Daniels managed the project and provided guidance based on extensive cryocooler experience. Mr. Michael Goldowsky contributed invaluable mechanical and electro-mechanical design insight. Dr. Chi Keung performed thermodynamic and electromagnetic numerical analysis and optimization as well as design. Mr. Bruno Smits and Mr. Joseph Hejduk contributed innumerable design detail improvements during the development of the detailed layout drawing. The entire Mechanical Systems technical staff reviewed the progress and offered helpful advice.

TABLE OF CONTENTS

LIST OF ILLUSTRATIONS

LIST OF TABLES

1. INTRODUCTION

This report covers Phase II of a program for the Office of Naval Research to determine whether the cooling required by a magnetometer, specified as 50 mW at 10°K, can be generated by a refrigerator having an efficiency, weight, and size compatible with military applications, i.e., relatively low power input, and comparatively light and small. The Phase I study, described in the report dated September 1980 and entitled "Design Study of Small Efficient Cryocoolers", resulted in the selection and preliminary layout of a Stirling cycle cooler having a triple-expansion free displacer and a compressor directly driven by a linear motor. During Phase II, the Phase I design was refined to arrive at an optimum combination of thermal, physical and operational characteristics. Details of that configuration are given in a final layout drawing which can serve as the basis for the preparation of manufacturing drawings.

2. DESIGN APPROACH

The Philips Stirling Optimization Program was used to optimize the Phase I design. The resulting output included thermodynamic specifications, some dimensions, and identification of some materials. Practical considerations of weight, reliability, complexity, material availability, and fabrication were then applied to perturb the theoretically optimized design. The perturbed designs were then analyzed thermodynamically with the Philips Stirling Evaluation Program. Throughout the design process, practical considerations and thermodynamic optimization were iterated to achieve the optimal, physically-realizeable cooler.

After the key characteristics of cold production and input power were optimized and subjected to practical design constraints, the resulting vibrations and electromagnetic interference (EMI) will be reduced by means external to the thermodynamic components. The vibrations will be attenuated by a tuned, passive, vibration absorber; the EMI will be attenuated by an external envelope of high-permeability magnetic shielding.

The design objectives are summarized in Table 1. The thermodynamic design values resulting from constrained optimization are listed in Table 2, and the cooler layout is shown in Figure 1.

The basic subsystems of the cooler are described in Section 3, viz., piston/motor, displacer, cold finger, vibration absorber, EMI shielding, and additional peripheral components.

TABLE 1. Design Objectives.

Cold production:	50 mW @ 10°K
Input power:	< 250 W
Weight:	minimize (25 kg goal)
Magnetic noise:	minimize (1.0 micro Gauss goal)
Vibrations:	minimize (goal of 0.1 micro-radian rotation of cold tip)
Cold tip temperature regulation:	fluctuations < 0.01°K
Cooldown time:	< 24 hours

TABLE 2. Thermodynamic Design Values.

Mean pressure:	0.49 MPa (4.84 atm)
Speed:	8.33 Hz (500 cpm)
Piston amplitude:	45 mm (1.77")
Piston diameter:	46.5 mm (1.83")
Piston mass:	2.6 kg
Displacer amplitude:	3.73 mm (0.147")
Displacer phase shift:	52°
Displacer mass:	0.55 kg
Displacer spring stiffness:	14.5 kN/m (82.8 lbf/in.)
Expansion space temperatures:	10, 53, 105°K
Maximum pressure:	0.69 MPa (6.83 atm)
Minimum pressure:	0.34 MPa (3.37 atm)
Cold Production:	200 mW @ 10°K
Mechanical input power:	180 W

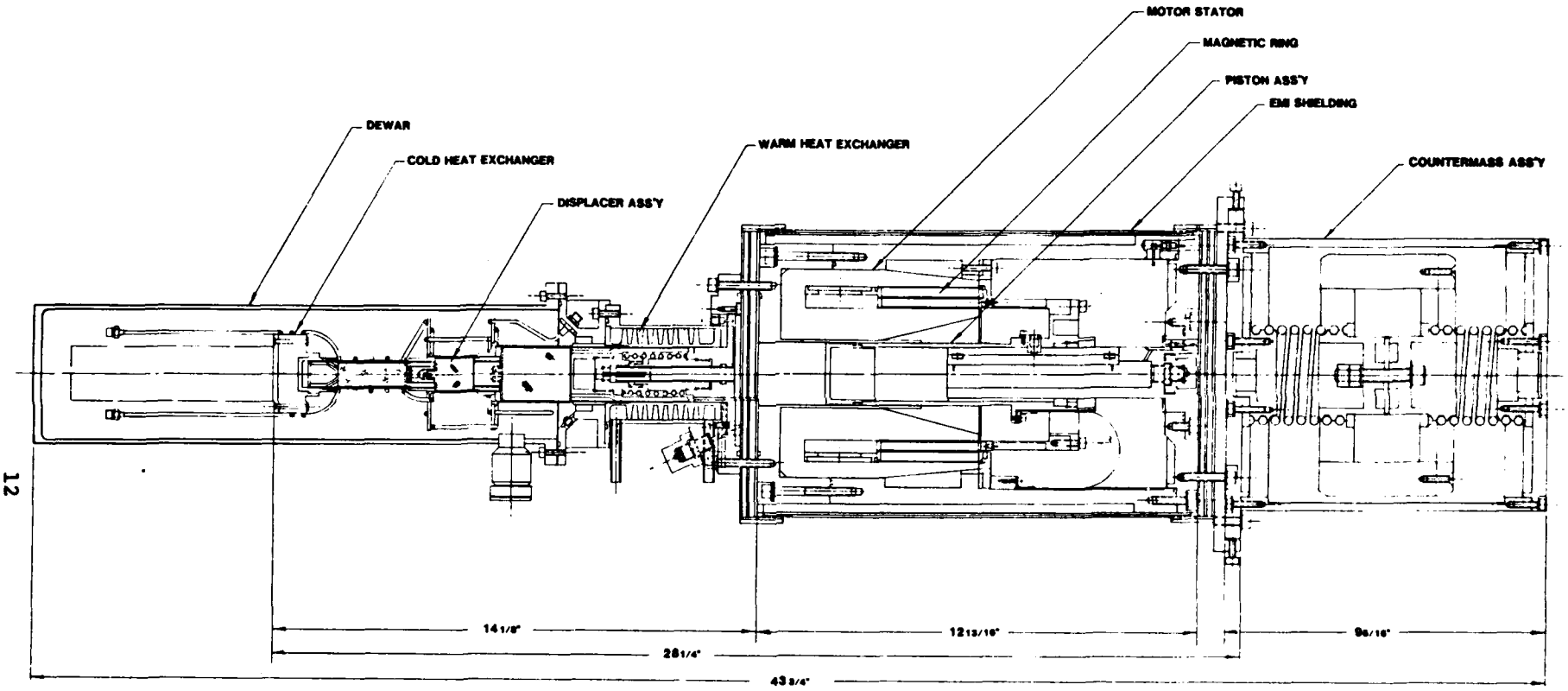

Figure 1. Layout drawing of 10°K Stirling cycle cooler.

3. SUBSYSTEM DESIGN

3.1 Piston/Motor

The piston assembly includes a cylindrical piston and a concentric, linear-motor armature to which the piston is rigidly attached. The piston is driven directly by a linear motor. The motor and its housing dominate the total weight of the thermodynamic components, and thus merit particular attention in their design. These components are shown in Figure 2.

The thermodynamic optimization requires that the piston sweep a volume of 76.0 cc, with a resultant pressure wave of 0.34 to 0.69 MPa. For optimal system efficiency with a linear drive motor, the diameter of the piston and mass of the piston assembly should be selected so that the assembly resonates with the spring force of the compression space, at the cooler speed. Also, to minimize compressor losses due to transient heat transfer, the surface area of the compression space should be minimized. This requires the piston amplitude to be approximately equal to the piston diameter.

With these mass and dimensional constraints, the linear drive motor was designed for minimum weight and maximum efficiency. For high efficiency, selection of stator magnet material is based on maximizing the energy product; samarium cobalt was the clear choice. For low weight and high efficiency, the stator yoke material should have high saturation flux density at low reluctance and high electrical resistivity, respectively. Vanadium Permendure (49 Co, 49 Fe, 2 V) was the best available material. Although Permendure is not available in bulk form in the dimensions required for the stator, the stator could be fabricated from six segments of available 4 in. diameter Permendure bar stock. Also, it might be possible to forge, recast, or powder-compact the stator from available Permendure stock.

The geometry and dimensions of the motor were optimized with finite-element mappings of the stator and gap flux densities for various layouts of selected magnetic materials. The finite-element, magnetic-field program permitted the inclusion of analytically intractable effects such as non-linear hard and soft magnetic materials, saturation, and leakage. A plot of the flux density for the final design is shown in Figure 3. Eddy current losses are reduced by laminating the stator with radial cuts. The

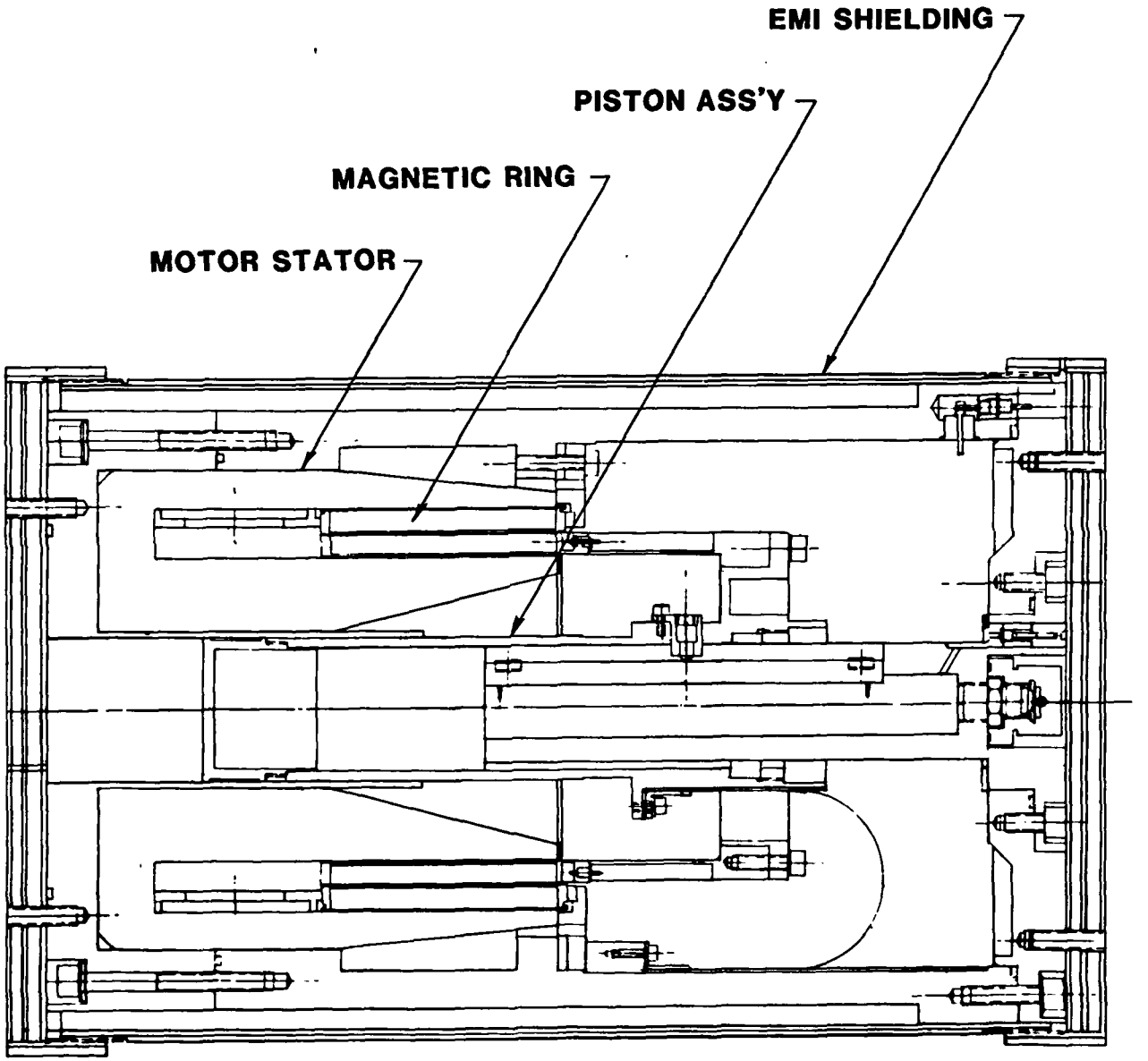

Figure 2. Layout drawing of piston/motor section.

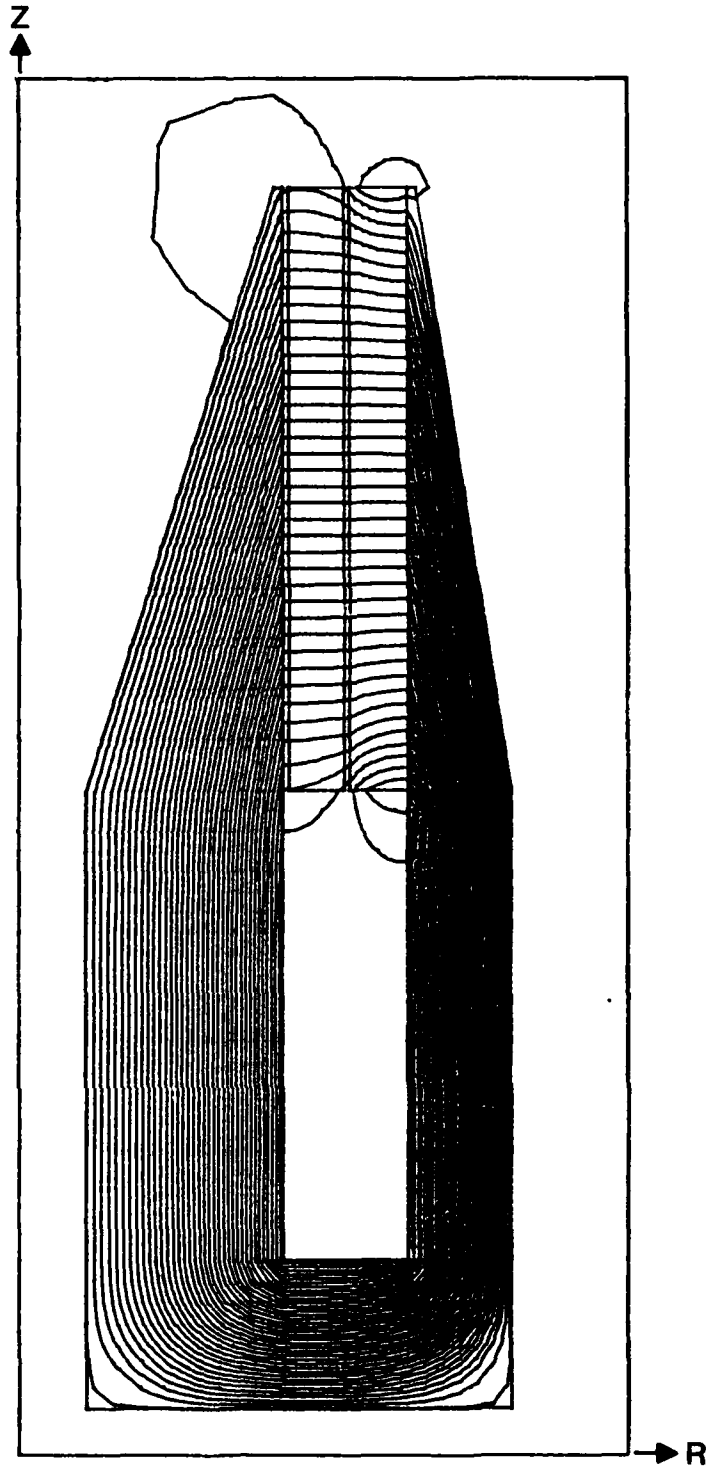

Figure 3. Flux plot of motor stator.

magnetic analysis resulted in an improved motor design with lower weight and higher efficiency than that of the preliminary design of Phase I. The motor design values are given in Table 3.

TABLE 3. Motor Design Values.

		Stator	
Magnets:	Material		$samarium_3cobalt$
	Energy product		160 kJ/m^3 (20 MG-Oe)
	Magnetic ring		
	Dimensions:	Axial length	72.5 mm
		Inside diameter	105.3 mm
		Outside diameter	127.3 mm
Yoke:	Material		vanadium Permendure
	Stator flux density		2.1 Tesla
	Gap flux density		0.45 Tesla
	Laminations:		Radial wire EDM slits, 0.381 mm (0.015")
			50 slits from radius 25 mm to 50 mm
			100 slits from radius 50 mm to 76 mm
		Armature	
Coil:	No. of turns		336
	Resistance		1.54 ohms
	Inductance		71.0 mH
	Peak current		4.4 A
	Peak voltage		87 V
	Electrical input power		192 W
	Mechanical output power		175 W
	Efficiency		91%
	Dimensions:	Axial length	72.5 mm
		Inside diameter	98.2 mm
		Outside diameter	105.0 mm

To minimize the side loads on the piston seal and bearings and to meet the mass requirement for the piston assembly, a moving-coil rather than moving-magnet motor design was chosen. Power transfer to the moving coil throughout its relatively large excursion is accomplished with rolling leads consisting of strips of 0.127 mm (0.005") beryllium copper, 10 mm wide and 135 mm long. The strips are guided along parallel surfaces: a stationary surface on the housing inside radius and a moving surface on the piston assembly. The strip deforms in a circular arc of radius 28 mm between the guides. During operation, the moving circular deformation results in an acceptable peak oscillating stress of 275 MPa (40,000 psi), nonreversing.

The long piston excursion also influences the design of the piston position controller and the design of the piston bearings. The center position of the piston motion is commonly maintained with a mechanical spring. However, for sufficient stiffness with acceptably low internal stress over the entire piston displacement, such a spring would have to be unreasonably long. Therefore, the piston motion is controlled with position feedback to the motor drive amplifier. An optical transducer was selected as the position sensor; this choice results in adequate linearity with minimum transducer length. The stationary optical sensor detects a moving light emitting diode (LED) attached to the piston assembly. The LED current is supplied through rolling leads identical to those of the armature coil.

The piston seal and bearings consist of thin layers of Rulon (a reinforced Teflon) bonded to the contacting surfaces of the piston assembly. The piston head is a removable cap with a circumferential layer of Rulon about its outer diameter. The Rulon is very thin, about 0.13 mm (0.005"), to minimize wear and thermal expansion mismatches. The Rulon surface, sliding along the cylindrical wall of the compression space, acts as a bearing as well as a seal.

A second bearing at the opposite end of the piston assembly also consists of a Rulon surface sliding on a guide. For this bearing, the Rulon is bonded to the inner diameter of a removable, titanium, ring insert. The Rulon on this insert rides on a stationary concentric guidepost. The bearing and post are keyed to prevent rotation of the piston assembly. To minimize maintenance downtime, both bearings are easily removable and replaceable with interchangeable parts.

The piston assembly is made of titanium to minimize armature weight and to match the thermal expansion of the Permendure motor stator. The motor stator is piloted in a titanium flange which forms both the compression space cylinder and part of the exposed motor housing. For compatibility of thermal expansion, the rear bearing guidepost is also titanium. Shock pads located at both extremes of the stroke prevent damage during transit or in the event of overstroke during operation. The remainder of the motor housing is made of aluminum for low weight, low cost, and ready availability of material in the required dimensions. All motor housing joints include reusable metal C-rings for low leakage and for ease in disassembly and reassembly.

The overall piston/motor design is similar to earlier Philips designs. The practical considerations and performance expectations were guided by past experience with prototype linear motors for Stirling cryocoolers.

3.2 Displacer/Regenerator

The displacer and regenerator are the most critical components of a Stirling cycle cooler. The displacer in this cooler has three stages of regeneration with three corresponding expansion spaces. The regenerators oscillate as an integral part of the displacer. The displacer is not independently driven, but oscillates with a mechanical spring in response to the compressor pressure wave. The displacer must be designed for the optimal compromise among the conflicting requirements of flow pressure drop, internal heat transfer, and thermal energy storage. The regenerator must be designed for efficient transient gas-solid heat transfer, yet have low conduction heat leak and low flow losses. The transient heat transfer and thermal energy storage must be compatible with the charge pressure and speed of the cooler. The above requirements dictate an optimal displacer amplitude and phase shift relative to the piston. Furthermore, practical requirements, such as reasonable length, weight, and reliability, must be met. The regenerator design requires special attention, because regenerator losses account for the majority of the thermodynamic losses.

The regenerator material of each stage is contained within a thin titanium can. The wall thickness of the can is 0.762 mm (0.030") for the first (warmest) regenerator and 0.508 mm (0.020") for the second and third regenerators. The regenerators are linked together axially with flexible connections. The material and packing configuration of the regenerator are optimized with respect to the effects of axial heat leak, fluid-to-regenerator heat transfer, regenerator heat capacity, fluid flow losses, and dead volume. The resulting design values are listed in Table 4.

Rulon bearing/seal surfaces similar to those of the piston are used at the two link locations and at the warm end of the first (warmest) regenerator. These seals will not be as easily replaceable as the piston seals. Such replacement, however, will be infrequent because the displacer seals will have a lower wear pressure and a much lower wear velocity. Furthermore, some leakage past partially worn regenerator seals will not have a serious

TABLE 4. Regenerator and Heat Exchanger Design Values.

Regenerators

Temperature (°K)	10	55	105
Type	lead spheres	phosphor bronze mesh	phosphor bronze mesh
Length (mm)	50.0	27.2	50.0
Area (sq. mm)	227.0	452.0	1163.0
Fill factor	0.63	0.42	0.34
Sphere or wire dia. (mm)	0.135	0.041	0.041

Heat Exchangers

Temperature (°K)	10	300
Gap (mm)	0.10	0.30
Length (mm)	10.0	51.5
Circumference	56.5	126.0

effect, since the pressure drop across the seals is low, and the leakage flow will experience some gap regeneration in the displacer clearance space.

Lead was chosen as the third-stage regenerator material because of its ability to maintain its heat capacity at low temperatures. Lead spheres appear to be slightly more efficient than lead mesh, but are less durable. Lead mesh could still be substituted for the spheres.

In addition to containing the regenerators, the displacer is also an integral part of the heat exchangers. At the warm end, the displacer has a cylindrical shell extension which forms a narrow gap passage for the helium working fluid. This gap between the outer diameter of the displacer extension and the inner diameter of a forced-liquid ambient heat exchanger forms the heat transfer surface for rejection of the heat of compression of the working fluid. The liquid side of the warm-end heat exchanger consists of a fluid channel which spirals about the circumference of an aluminum cylinder. The cooling fluid is hermetically isolated from the working space of the machine. The design values for the warm-end heat exchanger

are listed in Table 5. The external cooling fluid was assumed to be water, though other fluids are acceptable. The cooling fluid may be recirculated or run open-cycle.

TABLE 5. Ambient Heat Exchanger Design Values (Forced Water Cooling).

Heat exchanger material	aluminum
Channel cross-sectional area	41.2 mm^2
Mean channel helix diameter	56.0 mm
No. of channel turns	8
Flow rate	3 liters/min (50 cc/sec)
Pressure drop	20.0 kPa (2.9 psi)
Heat removal rate	250 W
Fluid temp. rise (inlet to outlet)	1.2°K
Fluid to channel ΔT	2.5°K

At the cold end, the cylindrical extension of the displacer is an integral part of the second gap heat exchanger which transfers heat from the device to be cooled to the working fluid. For damping variations in temperature, the heat exchanger has a lead and copper cap (see Sect. 3.3).

The displacer with its three regenerators moves as a single unit out of phase with the piston. The displacer has no independent driver; its motion is determined by the compression pressure, the expansion space pressures, the helium-flow pressure drop through the regenerators, the bearing friction, the displacer mass, and the displacer spring stiffness. These factors are adjusted to achieve the optimal displacer amplitude and phase lag. To compensate for fabrication tolerances and computation inaccuracies, the displacer has an adjustable spring stiffness and adjustable tuning mass. A linear variable differential transformer (LVDT) monitors the displacer position. The signal from this transducer can be used to measure the displacer amplitude and phase shift in order to optimize the mass and spring stiffness. The LVDT is packaged concentric with the mechanical spring and thus adds no additional length or weight to the machine.

The displacer design draws on Philips' proven experience with both commercial and experimental free-displacer and triple-expansion-displacer machines. The performance expectations of the present design are, therefore, justified both theoretically and empirically.

3.3 Cold Finger

The cold finger and Dewar are shown in Figure 4. The cold finger is the thin pressure vessel which contains the displacer. It must be thin to minimize the heat leak from the warm end of the cold tip, yet have the structural integrity to support the mass of the displacer, the cold-tip heat exchanger, and the device to be cooled. Also, it must contain a varying pressure of helium without fatigue and not be excited in any vibration modes due to the displacer dynamics. For low heat leak and high mechanical strength, the cold finger is made of titanium. The titanium wall thickness is 0.020" at the third (coldest) stage, 0.020" at the second stage, and 0.030" at the first stage. Between stages where the diameter is reduced, the bearing surface of the displacer is reinforced with heavy titanium rings. For the design dimensions and materials, a conservative stress analysis predicts:

- Lowest mode frequency: > 100 Hz
- Worst case deflection due to all masses: < 0.01 mm
- Hoop stress from peak pressure: < 27 MPa (4,000 psi)

All joints from the cold tip to the warm-end heat exchanger are hermetic TIG welds or brazes. The joint between the displacer and piston sections is sealed with a reusable metal C-ring.

At the cold tip there is a copper and lead cap for damping temperature variations. The copper surfaces help to make the heat flux distribution more uniform throughout the lead. The lead provides a large heat capacity for thermal damping. The lead and copper are soldered at all interfaces to avoid contact resistance.

The mass of the lead is 500 g. Its thermal mass will attenuate the temperature variations to less than $\pm$ 0.01°K. Copper end caps and multiple axial copper pins through the lead help to reduce the conduction temperature gradient. The theoretical analysis can be found in Section 2.2.3 of the Phase I report; the fabrication details were established in Phase II.

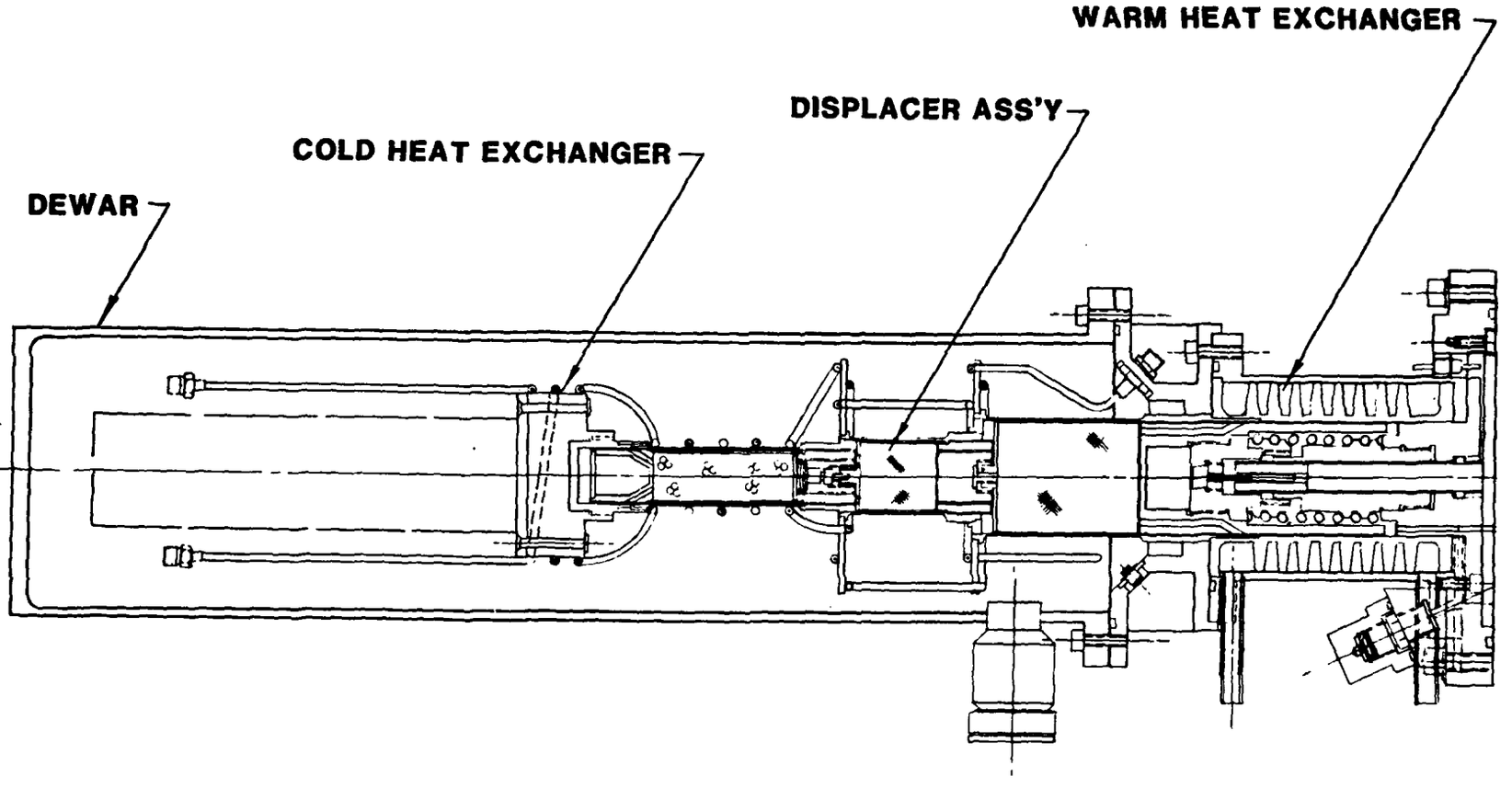

Figure 4. Layout drawing of displacer section.

Stainless-steel coaxial signal leads (Uniform Tubes UT-85SS), are used for connecting to the cryogenically cooled device which is attached to the end of the cold finger. The leads are cooled continuously along their length by coiling them about the cold finger in contact with the titanium wall. The leads are thus cooled to establish the same axial temperature gradient as the cold finger. Further, several turns of the leads are in thermal contact with two radial titanium disks extending from the first and second expansion spaces. These two disks act as heat exchangers for the leads as well as axial radiation shields.

The cold finger is enclosed by an evacuated Dewar. The Dewar housing is a vacuum-tight aluminum enclosure which remains at ambient temperature. Its interior surface is covered with layered superinsulation which provides radial radiation shielding with minimal conduction losses. The Dewar losses should be insignificant relative to the specified 50 mW cooling load.

The coaxial leads terminate in BNC connectors at the cold tip and in BNC feedthroughs at the Dewar wall near the warm-end heat exchanger. A helium fill valve is located near the piston/displacer interface. The Dewar housing is easily removed for access to the device and instrumentation.

3.4 Vibration Absorber

The linearly reciprocating motions of the piston and displacer give rise to an axial momentum imbalance. This imbalance can be compensated with a third mass oscillating in opposition. Such a mass in resonance with a linear mechanical spring will be excited to absorb vibrations at its natural frequency. If the piston and displacer oscillate sinusoidally at a constant frequency, then a tuned, passive spring/mass vibration absorber will sharply attenuate the imbalance forces. The effectiveness of this approach depends on:

- Imbalance occurring at a known fixed frequency.
- Precise tuning of the absorber resonance.
- Good spring linearity.
- Very low damping (high quality resonance).
- Characteristics of the machine mount.

Because the piston oscillates against the nonlinear gas spring of the compression space, the resulting piston motion is nonsinusoidal. The imbalance force is, therefore, composed of a large force at a fixed frequency plus superimposed higher harmonic imbalances. A passive absorber will attenuate only the imbalance at the fundamental frequency. For additional compensation, the cooler's position sensors can be used. The higher harmonics of the piston can be attenuated by using the optical sensor in position feedback to the piston motor to enforce pure sinusoidal motion. If further vibration attenuation is required, an active vibration compensator could be built to replace the passive design. An active compensator could use the displacer and piston position signals in feedback to the compensator's linear motor to inertially cancel any momentum imbalance.

A passive vibration absorber (see Fig. 5) was designed for this cooler. It is an external unit which bolts to the back plate of the motor housing, coaxial with the piston and displacer. Coaxial alignment is adjustable with positioning screws on the cooler baseplate. Resonance tuning is accomplished with a removable mass tuning ring on the moving countermass. Spring linearity is maintained with relieved helical spring mounts.

To insure low damping, the countermass bearings must have very low friction. This is accomplished by supporting the countermass only by its springs. With this approach, the only damping present is material damping in the springs, some friction between the springs and their mounts, and air damping. Since the countermass is not guided in linear bearings, it must be designed so that its various degrees of freedom do not have resonant frequencies close to the speed of the cooler. The degrees of freedom consist of axial translation, lateral translation, rotation about the machine axis, and a rotational rocking mode normal to the machine's axis. The design parameters of spring wire diameter, spring coil diameter, spring length, mass of the countermass, rotational inertia of the countermass, and rocking inertia of the countermass were selected to optimize the performance of the absorber. Optimization criteria included low spring stress, low weight, and separation of modal frequencies. The resulting design values are given in Table 6.

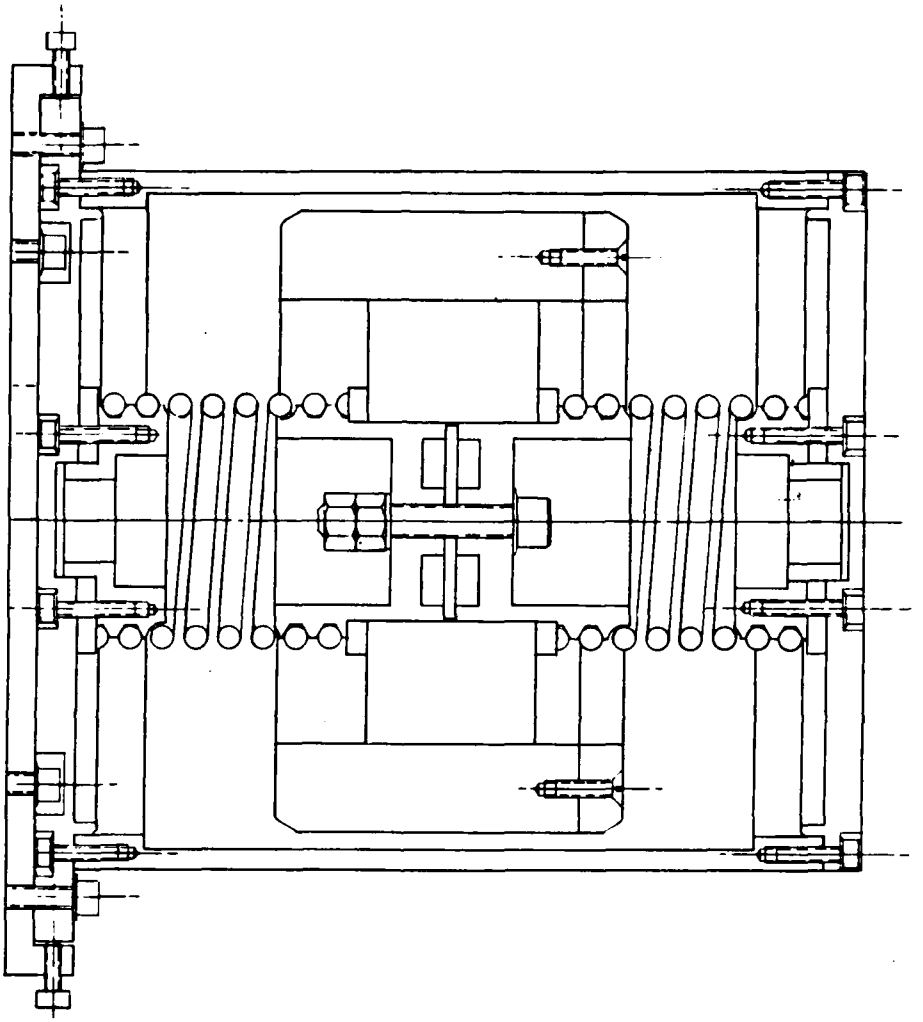

Figure 5. Layout drawing of vibration absorber.

TABLE 6. Vibration Absorber Design Values.

Springs (2): Each at,	
Total number of turns	7.5
Number of active turns	4.5
Wire diameter	6.35 mm
Material	music wire
Mean coil diameter	66.7 mm
Free length	71.4 mm
Active length	42.9 mm
Springs: Combined pair	
Combined axial stiffness	32.6 kN/m
Combined lateral stiffness	52.2 kN/m
Moving Mass:	
Mass	11.9 kg
Polar inertia	0.029 kg-m^2
Rocking mode moment of inertia	0.050 kg-m^2
Modal Frequencies:	
Axial transition	52.3 rad/sec
Laterial transition	66.2
Rotation about axis	22.5
Rocking mode	80.2
Operating Conditions:	
Peak force	350 N
Peak amplitude	11.0 mm
Peak spring stress	122.0 MPa (18,000 psi)

The total weight of the absorber unit is 17.0 kg. Since it is externally connected to the cooler, the absorber can be removed if not needed, replaced with an active unit if required, or transported separately if desired.

Because of the cooler's cylindrical symmetry, rotational deflections at the cold tip should be minimal. Such asymmetric deflections will only result from fabrication tolerances. Nonetheless, reducing the excitation due to pure axial momentum imbalances will reduce the mechanical vibration response in all modes, including cold finger rotations.

3.5 EMI Shielding

The dominant source of electromagnetic interference from this cooler is piston motor noise. The motor coil current which oscillates at 8.3 Hz induces a large time-varying magnetic field. This interference is attenuated by the surrounding motor stator, and further attenuated by shielding that encloses the piston motor. For a conservative calculation of shielding effectiveness, the stator attenuation was ignored. A two-dimensional, finite-element, magnetic field program was used to analyze the static field due to the peak current in the coil within the symmetric enclosure. Since the coil excitation is low frequency, shielding effectiveness is dominated by reluctance considerations rather than by eddy-currents; thus, a quasi-static analysis is valid.

Figure 6 shows a magnetic flux plot for one quadrant of the cross section of the motor coil in free space. There is rotational symmetry, as well as reflected symmetry, in the negative axial direction. Figure 7 shows the effect of placing thin, circular, magnetic discs over the front and back plates of the motor housing. The magnetic material chosen, Hipernom (Carpenter Technology Corp.) alloy, has a minimum permeability of 100,000 and a saturation flux density of 0.4 Tesla. Figure 8 shows the effect of enclosing the coil with a Hipernom cylindrical can connecting the two end plates. The peak field within the enclosure is 0.02 Tesla. The peak field within the 0.76 mm (0.030") thick shield is 0.24 Tesla. The peak field at the cold tip location is less than 0.1 micro Tesla. Additional layers of shielding material at the end plates produce further attenuation, but their influence is beyond the numerical accuracy of the field program. Multiple radial shielding layers for the cylindrical can will provide no additional attenuation of EMI at the cold tip.

The shielding design consists of a single layer of 0.76 mm (0.030") Hipernom supported by a shell of aluminum for the radial shielding, and multiple layers of Hipernom at the end plates for axial shielding. The end plates consist of three disk layers of 0.76 mm (0.030") Hipernom separated by two layers of 5 mm (0.200") copper. The separating copper disks provide an optimal reluctance gap as well as high-frequency eddy current shielding. Both end plates experience some leakage through bolt holes. The hole locations are placed off axis, as far as possible, to reduce the contri-

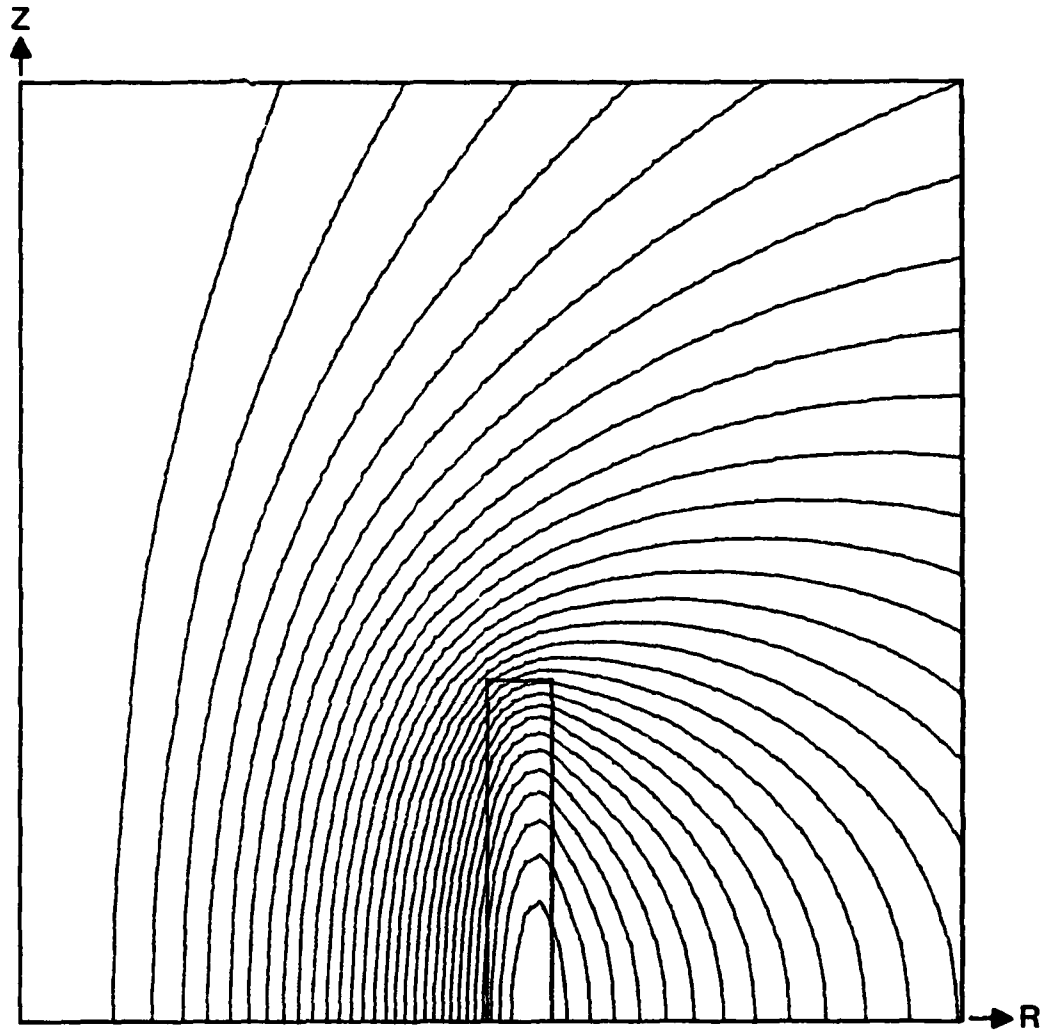

Figure 6. Flux plot of cylindrical coil in free space.

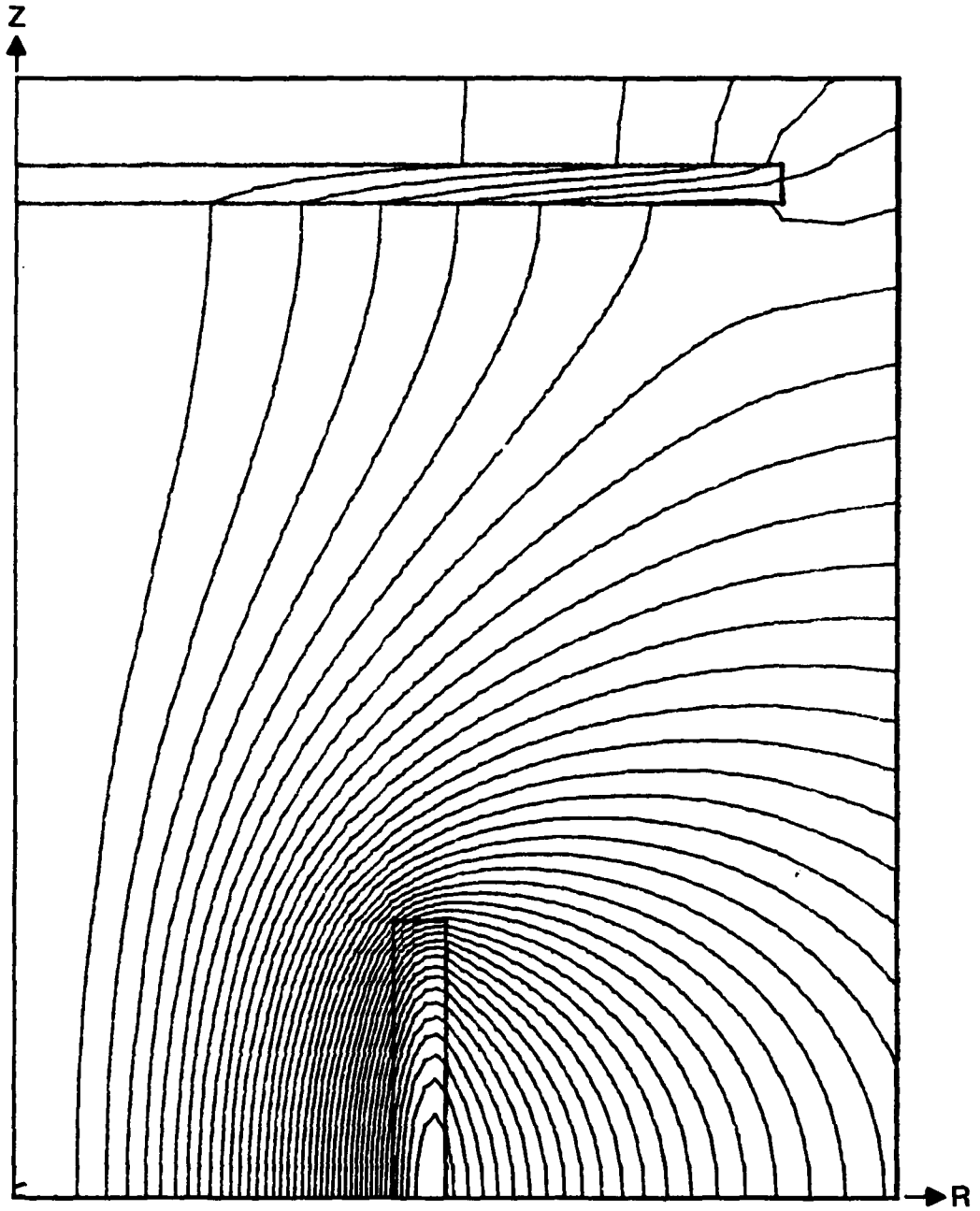

Figure 7. Flux plot of cylindrical coil with axial shielding disks.

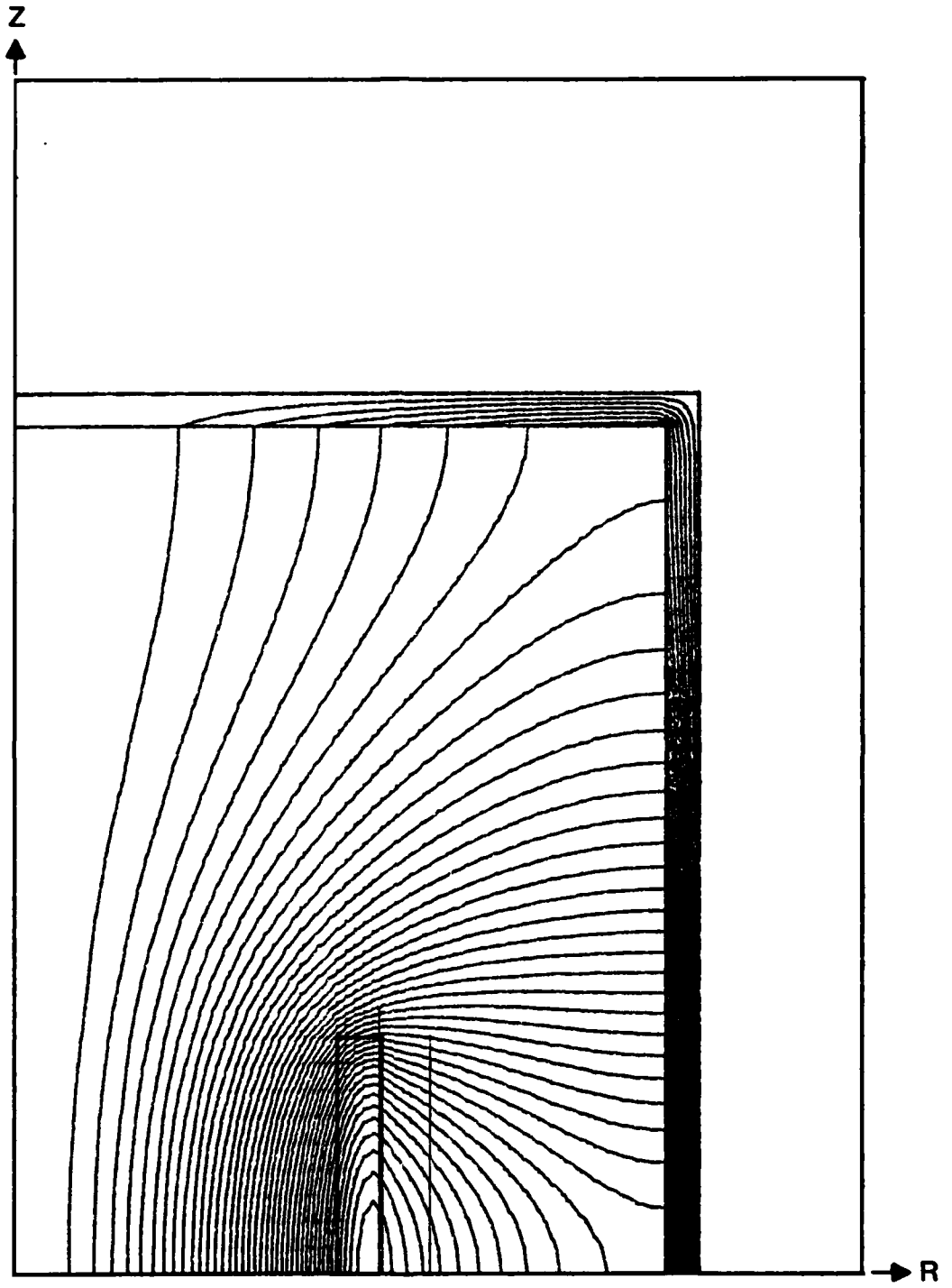

Figure 8. Flux plot of coil enclosed by magnetic shielding.

bution of this leakage to the magnetic noise at the cold tip. Also, the end plate between the motor housing and displacer section must contain gas passages for the helium to flow between the compressor and displacer. These passages have been designed to minimize the effects of magnetic leakage, additional compression dead volume, and helium flow losses. The resulting manifold consists of 16 axial holes with a diameter of 2.38 mm (3/32"), each placed 19.0 mm off axis. This design results in less than 2 W of flow losses.

The radial shielding has a low reluctance connection to the end-plate shielding through a threaded contact. The rear end plate and cylindrical can are external, and thus easily removable from the cooler. The end plate which forms the manifold between the displacer and piston can be removed if it is replaced with a similar plate to form the gas manifold and seat the C-seals. Thus, the shielding can be increased if necessary or removed if not needed. Also, for purposes of portability in the field, the shielding can be removed and transported separately, without loss of the working fluid.

3.6 Peripheral Equipment

Peripheral support equipment for the cooler consists of motor driver electronics and an ambient, forced-convection cooling system. The piston motor requires a dc power supply of at least 200 V, 250 W. The motor driver is a pulse-width-modulated amplifier with some feedback circuitry. The amplifier can achieve a power transfer efficiency of 85%.

The cooling system is required to remove the heat of compression and the motor losses from the ambient heat exchanger. This can be accomplished with a closed-cycle recirculating bath, or with an open-cycle flow of any available liquid at ambient temperature. The flow requirements of 3 liters per minute through a pressure drop of 3 psi can be satisified with a small water pump consuming less than 5 W.

The warm-end heat exchanger could be redesigned for air cooling. However, the weight and power requirements would exceed those of a closed-cycle liquid cooling system.

The peripheral equipment is commercially available, although custom design would reduce power, weight, and size. This support equipment can be easily detached and transported separately.

4. DISCUSSION OF RESULTS

The given design meets or betters the goals for cooling and power consumption. Extensive effort was expended to minimize vibrations and EMI; the resulting noise, however, may not meet the demanding design goals. The total system weight is substantially higher than that of the goal; a weight breakdown is given in Table 7. The limiting factors and trade-offs are discussed below.

TABLE 7. Weight Summary.

Piston Side		
Motor stator	11.0 kg	
Magnet ring	1.6	
Piston assembly	2.6	
Motor housing	12.0	
Subtotal		27.2 kg
Displacer Side		
Displacer	0.55	
Cold finger	3.00	
Ambient heat exchanger	3.10	
Dewar	2.05	
Subtotal		8.70
EMI Shielding		
Aluminum	0.50	
Hipernom	1.30	
Copper	6.80	
Subtotal		8.60
Countermass		
Moving mass	11.90	
Housing & stationary mass	5.10	
Subtotal		17.00
Total		61.50 kg

The thermodynamic efficiency of the cooler is primarily limited by the regenerator efficiency. The responsible effect is the loss of specific heat of all materials at low temperature - a problem that has long been

recognized. An improvement in regenerator efficiency would require an impractical geometry for an operational cooler (excessively long displacer) or a breakthrough in materials development. Nonetheless, the current displacer design meets the specified thermodynamic objectives.

The cooler is intended for use with a superconducting magnetometer or gradiometer, mechanically attached to the cooler's cold finger and cooled by conduction. Since the device is passive, the net cooling load consists of heat conduction through the electrical leads and Dewar losses. The design requirement of 50 mW cooling at 10°K was established by measuring the coolant boil-off rate from an operating device submerged in liquid helium. Since the proposed cryocooler design has distributed cooling of the leads and a purged, evacuated Dewar with superinsulation radiation shielding, the actual net cooling load is expected to be significantly less. The cooler, however, will provide cold in excess of the prescribed 50 mW; specifically, 200 mW of cooling at 10°K at the maximum allowed input power of 250 W. By reducing the piston amplitude, the machine would provide the 50 mW of cooling with less than 100 W input power. For lower, steady-state cooling loads, the piston amplitude and corresponding input power requirements can be decreased even further. Conversely, at full power, the reserve cooling capacity can be used to accelerate the cooldown time. At 50 mW net cooling, the cooldown time is expected to be about six (6) hours.

The vibrations and EMI of the cooler were attenuated as far as practical with reasonable weight, size, power, and complexity. Additional attenuation could be achieved with added mass, active vibration compensation, more EMI shielding, active field compensation, or with a motor design stressing noise reduction rather than weight and efficiency. Each of these approaches involves penalties in system weight or power, for only a marginal reduction of noise.

Further noise attenuation could be accomplished through a major design revision. The cooler could be redesigned as a split system, allowing the compressor, the primary offending component, to be separated from the displacer. This approach also would involve some penalties in efficiency and weight.

The most simple option, if permissible to the constraints of the superconducting device, would be to run the cooler intermittently. Assuming 50 mW of excess cooling capability at 10°K decreasing to 0 W cooling at 8.5°K, the cooler could lower the temperature of the cold-tip thermal mass from 10°K to 9°K in roughly 60 seconds. Upon shutting off the cooler power, the vibrations and EMI noise generated by the cooler would cease. The heat leak through the regenerator matrix and stagnant helium, coaxial leads, cold finger wall, plus the Dewar losses, would cause the cold tip temperature to rise at a rate of roughly 2°K/minute. This would clearly not meet the desired temperature regulation of $\pm$ 0.01°K. However, a known, repeatable, smooth monotonic temperature ramp may be an acceptable disturbance subject to electronic compensation at the device output. This approach would satisfy the desired noise requirement and result in considerable weight savings, since the vibration absorber and EMI shielding could be eliminated.

5. FUTURE WORK

The detailed engineering design on this project is now completed to the extent that the next step would be the preparation of a drawing package from which an engineering prototype cooler could be fabricated. This phase, estimated at 6 months, would involve detailed drawings of individual parts, detailed tolerancing and preparation of manufacturing specifications, selection of commercial components, specification of assembly procedures, and final checking. In conjunction with the preparation of these drawings, any potential fabrication difficulties would be worked out on shop models, and tests would be conducted to confirm the design of the rolling leads and wear rates of the piston seal. No substantial changes are anticipated, however, as a results of these tests. The schedule for the subsequent fabrication and performance test of the working cooler is estimated at 14 to 16 months.

DISTRIBUTION LIST

Copies

(1) Scientific Officer
Director, Electronic & Solid State Sciences Program
Physical Sciences Division
Office of Naval Research
800 North Quincy Street
Arlington, Virginia 222217
Attn: Mr. Edgar A. Edelsack

(1) Administrative Contracting Officer
Defense Contract Administration Services
Management Area - New York
60 Hudson Street
New York, New York 10013

(6) Director, Naval Research
Laboratory, Attn: Code 2627
Washington, D.C. 20375

(12) Defense Technical Information Center
Bldg. 5
Cameron Station
Alexandria, Virginia 22314

(1) Office of Naval Research
Eastern/Central Regional Office
666 Summer Street
Boston, Massachusetts 02210

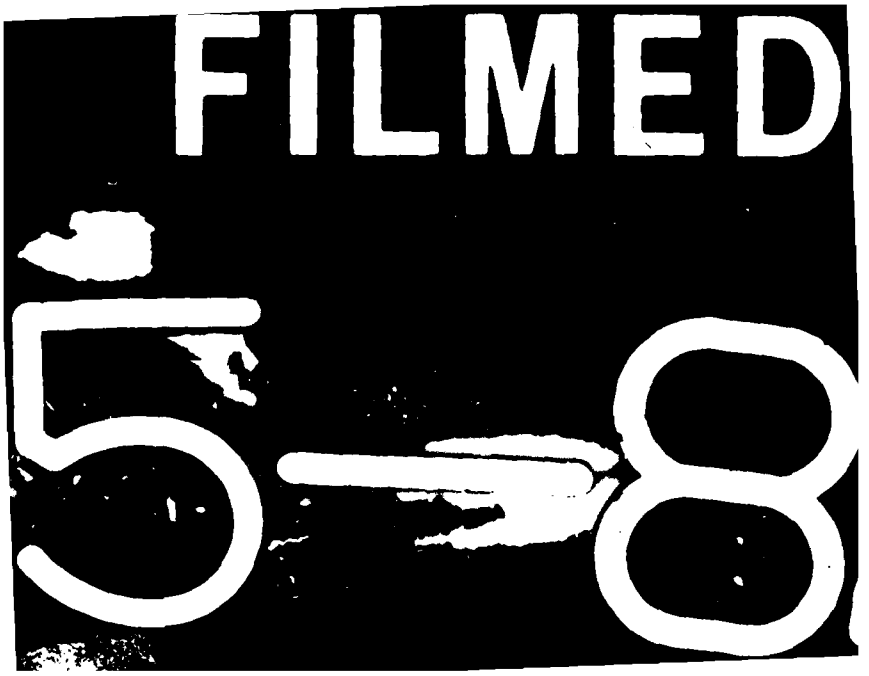
FILMED
5-8